Journal of Navigation and Port Research International Edition
Vol.31, No.9 pp. 785~791, 2007 (ISSN-1598-5725)

Numerical Analysis on Deformation of Submerged Structures using 2-Dimensional VOF-DEM Model

Mi-Kum Kim · †Chang-Je Kim***

** Department of Civil Engineering, Tottori University, Tottori, 680-8552, Japan*
***Division of Navigation System Engineering, Korea Maritime University, Busan 606-791, Republic of Korea*

Abstract : *In this paper we proposed a model that the deformation of the submerged rubble mound breakwaters composed with materials of various size, induced by wave action, can be computed. The water particle kinematics by waves in porous mound structure are computed by CADMAS-SURF, then the deformation of structure is computed using DEM module. To investigate the interaction of wave and sectional deformation of structures, analysis is accomplished by two steps. Analysis at the first step is executed with incipient mound. And analysis at the second step is executed with deformed mound by wave action. Furthermore, behaviors of materials are influenced by various properties such as the contact stiffness and the friction angle. Therefore, in order to present the behavior of the element caused by various properties, computations are accomplished with random coefficients by using the Monte Carlo simulation.*

Key words : *DEM, Rubble mound breakwater, CADMAS-SURF, Contact stiffness, Monte carlo simulation*

1. Introduction

In the numerical analysis on the deformation of submerged structures such as rubble mound breakwaters, the cavern formation process in sandy beaches, and the seabed liquefaction, Distinct Element Method (DEM), which has been proposed by Cundall, P. A. (1971), is recently used well. DEM has the essential applicability for analysis of fissured rock structures and discontinuous structures on seabed.

However, in the majority of previous studies on the deformation of submerged structures using DEM, elements of structures were assumed that it is composed of uniform size of materials(Araki et al., 2001; Araki et al., 2003), despite that actual submerged structures are constructed with various size materials, furthermore constant coefficients are adopted for calculation, despite that materials have various properties due to shapes, stiffness and friction angle. And the incident waves are assumed to be simple cyclic condition for the stable computation. As a result, analysis with assumed seabed or submerged structures is significantly different from those of actual states.

Also in the previous studies the interactions between the wave field and the sectional deformation of the structure have been rarely considered.

The goal of this study is to develop a new model for analysis of seabed deformation using discontinuous structures which consist of various size materials. As the first phase, we proposed a model that the deformation of the submerged rubble mound structures composed with various size materials can be computed.

The proposed model in this study has two sub-modules. One is wave computation module by CADMAS-SURF (Coastal Development Institute of Technology, 2001) based on VOF (Hirt et al., 1981) and SMAC method. And the other is structure computation module by DEM. In the wave module, Morrison model was adapted to determine wave forces.

In this study, we tried to compute the deformation of the rubble mound structure with various size materials on seabed and considered frictional resistance between seabed and rubbles by constructing seabed with regular size materials and concurrently presented pervious action to seabed by moving of rubble mounds due to wave force. To investigate the interaction of wave and sectional deformation of structures, analysis is accomplished by two steps. Analysis at the first step is executed with incipient mound. And analysis at the second step is executed with deformed mound by wave action. Furthermore, behaviors of materials are influenced by various properties of them, for example, shape of material, contact stiffness, friction angle etc.. Therefore, in order to present various behavior caused by various properties, computation is accomplished with random coefficients by Monte Carlo simulation for contact stiffness

* ddochi-77@hanmail.net 051)410-4226
† Corresponding Author : Chang-Je Kim, kimc@hhu.ac.kr (051)410-4226

and friction angle.

2. WAVE ANALYSIS

2.1 Reproduction of wave field

In this study, for computation of wave field, CADMAS-SURF is accepted. CADMAS-SURF is useful tool to compute the time and space variations of free surface based on VOF and SMAC method. Furthermore, CADMAS-SURF can be applied on the analysis of special topographical feature such as sloping surface of seabed and porous structures. The governing equations of CADMAS-SURF, which are the continuity equation for 2-D incompressible inviscid fluid and expanded equations on the basis of porous model with the Navier-Stokes equation , are given as follows:

$$\frac{\partial \gamma_x u}{\partial x}+\frac{\partial \gamma_z w}{\partial z}=S_p \tag{1}$$

$$\lambda_v\frac{\partial u}{\partial t}+\frac{\partial \lambda_x uu}{\partial x}+\frac{\partial \lambda_z wu}{\partial z}=-\frac{\gamma_v}{\rho}\frac{\partial p}{\partial x}+\frac{\partial}{\partial x}\left\{\gamma_x \nu_e\left(2\frac{\partial u}{\partial x}\right)\right\} +\frac{\partial}{\partial z}\left\{\gamma_z \nu_e\left(\frac{\partial u}{\partial z}+\frac{\partial w}{\partial x}\right)\right\}-D_x u+S_u-R_x \tag{2}$$

$$\lambda_v\frac{\partial w}{\partial t}+\frac{\partial \lambda_x uw}{\partial x}+\frac{\partial \lambda_z ww}{\partial z}=-\frac{\gamma_v}{\rho}\frac{\partial p}{\partial z}+\frac{\partial}{\partial x}\left\{\gamma_x \nu_e\left(2\frac{\partial w}{\partial x}+\frac{\partial u}{\partial z}\right)\right\} +\frac{\partial}{\partial z}\left\{\gamma_z \nu_e\left(2\frac{\partial w}{\partial z}\right)\right\}-D_z w+S_w-R_z-\gamma_v g \tag{3}$$

where, t is time, x and z are the horizontal and the vertical, u and w are the velocities of horizontal and vertical of the flow, ρ is the density, p is the pressure, ν_e is sum of the molecular dynamic viscosity and the eddy dynamic viscosity, g is the gravitational acceleration, γ_v is the porosity, γ_x and γ_z are the area transmittances of horizontal and vertical directions, $\lambda_v=\gamma_v+(1-\gamma_v)C_M$, $\lambda_x=\gamma_x+(1-\gamma_x)C_M$, $\lambda_z=\gamma_z+(1-\gamma_z)C_M$, C_M is inertia coefficient. And D_x and D_z are coefficients on damping area of energy, S_p, S_u and S_w are the source terms for wave source. And resistance from porous structure, R_x and R_z , are expressed as follows:

$$R_x=\frac{1}{2}\frac{C_D}{\Delta x}(1-\gamma_x)u\sqrt{u^2+w^2} \tag{4}$$

$$R_z=\frac{1}{2}\frac{C_D}{\Delta z}(1-\gamma_z)w\sqrt{u^2+w^2} \tag{5}$$

where, C_D is the drag coefficient, Δx and Δz are the cell intervals of direction x and z.

Advection equation of F, relational algebra of VOF, based on porous model is given as follow:

$$\gamma_v\frac{\partial F}{\partial t}+\frac{\partial \gamma_r uF}{\partial x}+\frac{\partial \gamma_z wF}{\partial z}=0 \tag{6}$$

2.2 Computation of wave force

Wave forces to elements are calculated as follows:

$$F_d=\frac{1}{2}\rho A C_D U_D|U_D| \tag{7}$$

$$F_i=\rho V C_M \dot{U}_D \tag{8}$$

$$F_l=\frac{1}{2}\rho A C_L U_D^2 \tag{9}$$

where, F_d is the drag force, F_i is the inertia force, F_l is the upward force, ρ is the density of a fluid, A is the area of projection, U_D is the relative velocity vector of element and fluid, V is the volume of element and $\dot{U}_D$ is the acceleration vector.

3. STRUCTURE ANALYSIS

Described model herein is a two-dimensional model (Kiyama et al., 1988). The driving forces are gravity and wave force. The solution algorithms are briefly described in following section.

3.1 Outline of DEM

In DEM analysis, rocks are treated as the rigid and elastic body, and non-elastic property of rock is expressed by inserted elastic spring with the contact coefficient K and cohesion dashpot with the damping coefficient η into contact point between rocks. Then, the equations of translation motion X and rotational motion ϕ of the one rock with mass m and the inertial moment I are expressed as follows:

$$m\ddot{X}+\eta\dot{X}+KX=0 \tag{10}$$

$$I\ddot{\phi}+\eta r^2\dot{\phi}+Kr^2\phi=0 \tag{11}$$

where, X denotes displacement with vectorial property and r is radius of rock.

These equations denote the diminish violation. And analysis

of the rock motion from movement to stillness is possible by computing the equations of motion for all rocks. But, generally, it is difficult to solve Eq. 10 and Eq. 11, simultaneously, because a rock contacts with several rocks and the unknown displacement, $\triangle x$, $\triangle z$ and ϕ are contained implicitly. Therefore Cundall(1971) proposed the progressional solution method by differential approximation using time step $\triangle t$ in Eq. 10 and Eq. 11 and by approximation of the equation which the unknown displacements are contained explicitly. For example, Eq. 10 is represented as follow.

$$m[\ddot{X}]_t = -\eta[\dot{X}]_{t-\triangle t} - K[X]_{t-\triangle t} \tag{12}$$

And then the equation is calculated by the assumption that new acceleration $[\ddot{X}]_t$, which new displacement $[X]_t$ is calculated by integral of $[\ddot{X}]_t$, is the explicit relational algebra of force at contact on the basis of displacement $[X]_{t-\triangle t}$ at the last step.

3.2 A two-dimensional simulation

In DEM analysis with a number of the polygonal elements, contact judgment is very difficult and the time for calculation is increased. On the other hand, in case of using the circular elements, be able to greatly increase in efficiency. In this study, DEM analysis with circular elements is performed.

1) Contact judgment and relative increment of contact

The state of contact between two elements i and j is judged by the relation between the positions (x_i, z_i) and (x_j, z_j) of each elements, the magnitudes of radius r_i and r_j, and distance R between each elements, as follows:

$$r_i + r_j \geq R_{ij} \tag{13}$$

$$R_{ij} = \sqrt{\{(x_i - x_j)^2 + (z_i - z_j)^2\}}$$

When the condition in Eq.(13) is satisfied, it is considered that two elements are contacting.

2) Relative increments of contact

When two elements, i and j, are approaching, the increments of relative displacement to tangential direction and normal direction during $\triangle t$, $\triangle X_n$ and $\triangle X_s$, are calculated as follows:

$$\triangle X_n = (\triangle x_i - \triangle x_j)\cos\alpha_{ij} + (\triangle z_i - \triangle z_j)\sin\alpha_{ij} \tag{14}$$

$$\triangle X_s = -(\triangle x_i - \triangle x_j)\sin\alpha_{ij} + (\triangle z_i - \triangle z_j)\cos\alpha_{ij} + (r_i\triangle\phi_i + r_j\triangle\phi_j) \tag{15}$$

where, $\triangle x_i$, $\triangle z_i$ and $\triangle\phi_i$ are the displacement increments of element i from time $t-\triangle t$ to t, α_{ij} is the angle between common normal and axis x, anti-clockwise rotation is positive.

$$\sin\alpha_{ij} = -(z_j - z_i)/R_{ij} \tag{16}$$

$$\cos\alpha_{ij} = -(x_j - x_i)/R_{ij}$$

3) Contact force

Contact force between i and j is classified into two forces. One is the compressive force f_n in normal direction. The other is the shear force f_s (clockwise on i is positive).

Increments of contact forces are given by Eq.(17).

$$\triangle e_n = K_n \times \triangle X_n \tag{17}$$

$$\triangle d_n = \eta_n \times \triangle X_n/\triangle t$$

where, K_n is the contact stiffness and $\triangle X_n$ is the relative displacement increment and $\triangle X_n/\triangle t$ is the relative displacement velocity. Herein, the compressive force is positive. Therefore, the elastic drag $[e_n]_t$ and the viscosity drag $[d_n]_t$ to normal direction at t are given by:

$$[e_n]_t = [e_n]_{t-\triangle t} + \triangle e_n \tag{18}$$

$$[d_n]_t = \triangle d_n$$

With negleting the tensile strength between elements, following conditions are added.

$$\text{In case of } [e_n]_t < 0,\ [e_n]_t = [d_n]_t = 0 \tag{19}$$

By the above, the compressive force $[f_n]_t$ in normal direction between two elements at t is calculated as:

$$[f_n]_t = [e_n]_t + [d_n]_t \tag{20}$$

As the case of normal direction, $\triangle e_s$ and $\triangle d_s$ are expressed as follows:

$$\Delta e_s = K_s \times \Delta X_s \tag{21}$$

$$\Delta d_s = \eta_s \times \Delta X_s / \Delta t$$

Therefore, the elastic drag $[e_s]_t$ and the viscosity drag $[d_s]_t$ to tangential direction at t are changed to following equations. Anti-clockwise on i is positive.

$$[e_s]_t = [e_s]_{t-\Delta t} + \Delta e_s \tag{22}$$

$$[d_s]_t = \Delta d_s$$

Considering the condition of Eq.19 and friction, three conditions are added as follows.

Non-contact condition: in case of $[e_n]_t < 0$,

$$[e_s]_t = [d_s]_t = 0 \tag{23}$$

The condition for friction: in case of $|[e_n]_t| > \tan\phi [e_n]_t$,

$$[e_s]_t = \tan\phi [e_n]_t \times SIGN([e_s]_t) \tag{24}$$

$$[d_s]_t = 0 \tag{25}$$

where, ϕ is the friction angle between elements, $SIGN(Z)$ is the sign of variable Z.

These conditions mean that the shear deformation is caused by the friction between elements. And Eq.23 denotes the non-contact condition and Eq.24 and Eq.25 denote the limit of friction force.

Finally the shear force in tangential direction at t, $[f_s]_t$, is calculated as follows.

$$[f_s]_t = [e_s]_t + [d_s]_t \tag{26}$$

3.3 Improvement of efficiency for contact judgment

The contact judgment is improved in order to reduce the run-time of computation. First, the whole calculation area is divided into equal small section, that is, the ranges of $0 \le x \le a$ and $0 \le z \le b$ are divided into m and n sections, respectively. Then, the section number of center $G(x, z)$ of element is investigated using the following equation.

$$N = m \cdot FIX\left[\frac{z_i}{b/n}\right] + FIX\left[\frac{x_i}{a/m}\right] + 1 \tag{27}$$

where, FIX denotes to make the integer by cutting the below of decimal point. By this calculation, the section number of i is decided. The section containing j with the possibility on contacting to i is restricted with one section containing j and eight adjacent sections. Then, when the detailed contact judgment for elements $j(\neq i)$ i nine sections is carried out, simple and speedy calculation is realized.

3.4 Coupling of DEM and VOF

Coupling of DEM and VOF is accomplished as Eq.(28) ~ Eq.(30) by adding the calculated wave force into the equations of motion of DEM.

$$(M_i + M_i')\ddot{x} = \sum_j [F_x]_{ij} + [f_x]_i \tag{28}$$

$$(M_i + M_i')\ddot{z} = \sum_j [F_z]_{ij} + [f_z]_i + v_i(\rho_p - \rho)g \tag{29}$$

$$(\phi_i + \phi_i')\ddot{\omega} = \sum_j [M_x]_{ij} \tag{30}$$

where, M_i and M_i' are mass and added mass of element i, $\ddot{x}$ and $\ddot{z}$ are acceleration components to direction x and z, $[F_x]_{ij}$ and $[F_z]_{ij}$ are contact forces from contacted element j , $[f_x]_i$ and $[f_z]_i$ are wave forces. And ϕ_i and ϕ_i' are the moment of inertia and the additional moment of inertia, v_i is volume of element, ρ_p is density of element, $\ddot{\omega}$ is angular acceleration to direction of each axis, $[M]_{ij}$ is moment to around each axis.

3.5 Monte Carlo simulation

Monte Carlo method, which is computation algorithms in terms of probabilities for simulating the behavior of physical phenomenon, is used to determine the values of the coefficients. In simulation by probability model, because each variation is uncertain, the variations are generated at random in accordance with probability distribution. In this study, in order to express the heterogeneous properties of materials of rubble mound, analysis is performed by Monte Carlo simulation and trial and error.

In DEM, because spring-dashpot model is introduced for computation, the important factors of behavior are coefficients which have connection with computation at contact such as contact stiffness, damping coefficient and friction coefficient. By changing the coefficients, similar behaviors to actuality are expressed. Generally, stiff material is expressed by inputting the large contact stiffness coefficient and speedy convergence is expressed by inputting the large damping coefficient. Therefore, bound rates of materials at contact

are controlled and behaviors of materials are traced.

In this study, the following method is adopted for random coefficient as damping coefficient, friction coefficient, etc. For example, damping coefficient is decided by following equation using random number.

$$\eta = \bar{\eta} + \bar{\eta} \cdot \sigma \cdot Z(i) \tag{31}$$

where, $Z(i)$ is random number, $\bar{\eta}$ is average of damping coefficient, σ is dispersion, given by

$$\sigma = \bar{\eta} \cdot \beta \tag{32}$$

where, β is standard deviation. Friction coefficient is also adopted by this method.

4. APPLICATION TO ANALYSIS

4.1 Making the incipient mound

In this study, a model test associated with deformation of submerged structure due to wave action was carried out. Computation area is depicted in Fig. 1. And the initial shape of mound is made as shown in Fig. 2. In Fig. 2, arrows denote water particle velocities and circles denote each elements of rubble mound. The mound is composed by 1500 elements with a radius of 1 cm, 300 elements with a radius of 2 cm and 300 elements with a radius of 1.5 cm. Making process of incipient model is simplified as follow. First, the seabed with regular size elements with a radius of 1 cm is composed. Then, the mound using elements with a radius of 2 cm and 1.5 cm is made by free fall. Although actual seabed is composed with smaller elements, elements with a radius of 1 cm are used for simplicity of computation.

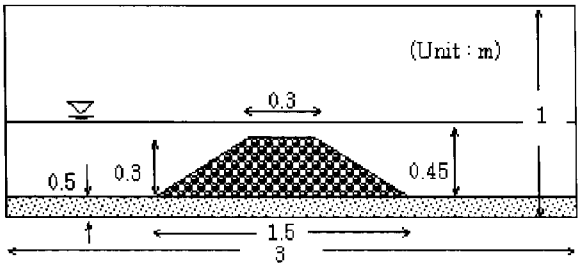

Fig. 1 Computation area

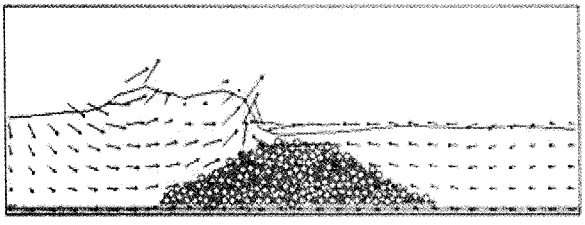

Fig. 2 Incipient model and wave profile for DEM analysis

4.2 Analysis of mound deformation at first step

First, in wave computation module, the CADMAS-SURF is adapted, and incipient mound model by DEM computation is used to compute the porous structure. For the porosity of the mound is set to be 0.38, according the previous study (Maeno et al., 2006). The computations are carried out with the wave height of 0.2m and the period of 2.0s. And the time interval Δt is 0.01.

In case of calculation by Morrison model, for the value of C_M and C_D, 1.5 and 0.5 are adopted, according to the formulary on hydraulics(Japan society of civil engineers, 1971).

Then, analysis on mound deformation is performed against the submerged breakwater model. Generally, the coefficients between elements such as the contact force and the damping coefficient are determined so as not inordinate repulsing and sinking. Therefore, the coefficients are determined by the method of trial and error. Furthermore, behaviors of materials are influenced by various properties, such as size, contact stiffness, friction angle etc., of them. Therefore, in this study, computation is accomplished with random coefficients determined by Monte Carlo simulation for contact stiffness and friction angle. The average value of each coefficient for Monte Carlo simulation is shown in table 1.

The results of DEM calculation at first step are shown in Fig. 3(a), 3(b) and Fig. 4. Fig. 3(a) shows the result with constant coefficients of Table 1. Fig. 3(b) shows the result with random coefficients by Monte Carlo simulation. Both results show the compacted deformation. From Fig. 4, the active movements of elements on the onshore side were found rather than the offshore side of the mound. But the discrepancy of deformation is not large.

Table 1 Input parameters for DEM calculation

Δt(s)	Calculation time(s)	Average of contact stiffness (N/m)	Average of friction angle (degree)
5×10^{-6}	15	1×10^{4}	30

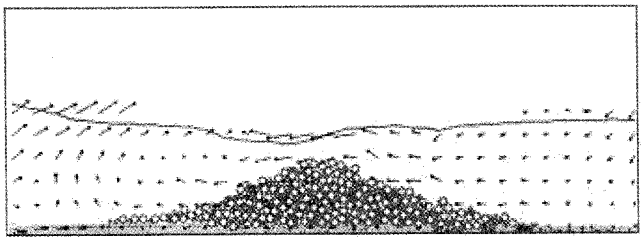

Fig. 3(a) Sectional deformation with constant coefficients and wave profile (15s)

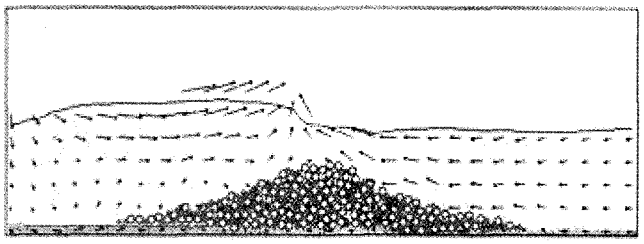

Fig. 3(b) Sectional deformation with random coefficients and wave profile (15s)

Fig. 4 Deformed section of mound after 15seconds

4.3 Analysis of mound deformation at second step

In this section, in order to investigate the interaction of wave and sectional deformation of the mound, the second analysis, which means the feedback to wave computation, is performed using the deformed mound by wave action in the first step. The wave conditions are same described in section 3.2. In the second step, 0.36 is adapted for the porosity of mound, because the elements were compacted by wave force at the first step.

Analysis on mound deformation was accomplished with deformed mound model, as shown in Fig. 3(a) and 3(b), and calculated wave force by Morrison model. Conditions of DEM computation in this section are equal to Table 1. The results of analysis are shown at Fig. 5(a), 5(b) and Fig. (6). The result of the deformation after 30s is diverged from the result of the deformation after 15s as shown in section 3.2. The depression at the onshore area of mound with condition of constant coefficients was shown clearly in Fig. 6. As a reason, we suppose that the depression at the onshore area is generated under the influence of undertow in the surf zone. However, in Fig. 5(b), the whole mound is compacted and the height of the crest is lower than Fig. 5(a).

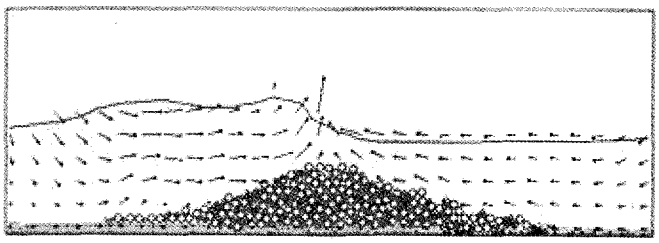

Fig. 5(a) Sectional deformation with constant coefficients and wave profile (30s)

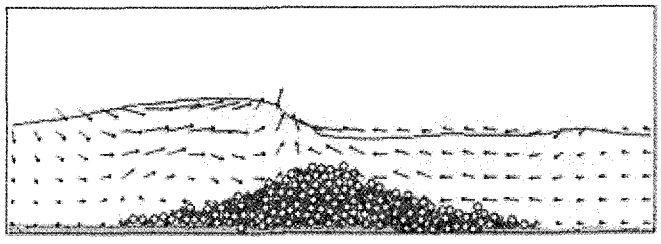

Fig. 5(b) Sectional deformation with random coefficients and wave profile (30s)

Fig. 6 Deformed section of mound after 30seconds

5. CONCLUSIONS

In this study, analysis on mound deformation caused by wave force was performed by coupling CADMAS-SURF and DEM. Wave was calculated by CADMAS-SURF against incipient mound by DEM analysis and wave force was calculated by wave velocities and Morison model. And deformation of mound was calculated by DEM. In DEM analysis, to consider the various properties of material, coefficients such as contact stiffness and friction angle are adopted the random value by Monte Carlo simulation. As a result, influence of interaction between wave and sectional deformation was expressed by the separated analysis into two steps. And the influences of various properties of materials are considered. But, reflection of the sequential interaction between sectional deformation and wave were not accomplished herein.

Hence, the model in this study is required some improvements such as to reflect the sequential interaction between deformation and wave and to advance the efficiency of computation. Furthermore, proof of the validity by comparison with result of experiment is required. By these improvements, more satisfactory analysis on deformation of structure is expected.

REFERENCES

[1] Araki, S., Kotake, Y., Kanazawa, T., Matsumura, A., and Deguchi, I. (2001), "Numerical simulation of deformation of rubble mound seawall with VOF and DEM", Proceedings of coastal engineering, JSCE, Vol. 48, pp.931-935.

[2] Araki, S., Yanagihara, T., and Deguchi, I. (2003), "Numerical simulation on 3-dimensional deformation of submerged breakwater with discrete element method", Proceedings of coastal engineering, JSCE, Vol. 50, pp.831-835.

[3] Coastal Development Institute of Technology (2001), "Research and development of CADMAS-SURF", No.12. (in Japanese)

[4] Cundall, P. A.(1971), "A computer model for simulating progressive, large-scale movements in blocky rock systems", Symposium on rock mechanics, Nancy, Vol.2, pp.129-136.

[5] Hirt, C. W. and Nichols, B. D. (1981), "Volume of fluid method for the dynamics of free boundaries", J. Comp. Phys., Vol.39, pp.201-225.

[6] Japan Society of Civil Engineers. (1971), Formulary on hydraulics, pp. 523. (in Japanese)

[7] Kiyama, H., Hujimura, H., and Nishimura, T. (1988), "Theoretical analysis of Fenner-Pacher type characteristic curves for tunneling by DEM", Journal of geotechnical engineering,394/II-9, pp. 37-44. (in Japanese)

[8] Maeno, S., Ogawa, M., and Bierawski, L. G.(2006), "Analysis on deformation of the permeable submerged breakwater by coupling of VOF, DEM and FEM", Annual conference of Coastal Engineering, JSCE, Vol. 53, pp.886-890.(in Japanese)

Received 4 December 2007
Accepted 30 December 2007